Available on CMS information server

CMS NOTE 2002/XXX

The Compact Muon Solenoid Experiment

CMS Note

Mailing address: CMS CERN, CH-1211 GENEVA 23, Switzerland

8 May 2002

Energy flow objects and usage of tracks for energy measurement in CMS.

D. Green

Fermi National Acceleration Laboratory, Batavia, Illinois, U.S.A.

O.Kodolova

CERN[a)]

I.Vardanian

Moscow State University, Moscow, Russia

A.Nikitenko[b)] and Tejinder Virdee

Imperial College, London, UK

S.Kunori

Maryland University, USA

Abstract

We present an algorithm to determine the energy of jets using the CMS calorimeter and tracker. The results on dijet mass reconstruction for $Z'(M = 120GeV) \rightarrow$jj events are presented. Improvement in Z' mass resolution when the energy flow objects are used is found to be about of 22 % in comparison with the usage of the calorimeter information only. We present also a method to improve jet energy resolution with the regional usage of the tracks when a jet is found first with a “standard” jet finder running on calorimeter towers as an input. We factorize the improvement in the jet energy resolution due to addition of tracks swept from the reconstruction cone in 4T magnetic field, and due to replacement inside cone of the cluster energy by the matched track momentum or (for bad matching) subtraction from the jet energy the expected response of the track in the calorimeter and adding to the jet energy the track momentum. It is shown that for the soft jets of $\simeq$ 30-40 GeV the energy resolution may be improved by about a factor of 2.

[a)] on leave from Moscow State University, Moscow, Russia

[b)] On leave from ITEP, Moscow

1 Introduction

A considerable improvement of the calorimeter jet energy resolution with the usage of the reconstructed tracks (energy flow algorithm) has been already demonstrated in a number of HEP experiments such as LEP [1], Tevatron [2], ZEUS [3], Tesla [4]. The possibility to resolve and identify calorimeter clusters with the fine transverse and longitudinal granularity of the calorimeter cells is one of the key features to obtain a big improvement of the resolution with the energy flow algorithms.

A first successful attempt to build the energy flow for the CMS calorimeter has been done in [5]. We will present an algorithm to build the energy flow objects and an updated results on dijet mass reconstruction for $Z' \rightarrow$jj events using these objects.

We also present a method to improve the jet energy resolution with the regional usage of the tracks when a jet is found first with a "standard" jet finder running on the calorimeter towers as an input. We factorize the improvement of the jet energy resolution and scale due to the addition of tracks swept out from the reconstruction cone by the 4T magnetic field, and due to cluster-track matching inside the jet reconstruction cone. For the bad track-cluster matching inside the cone we subtract from the jet energy the expected response of the track in the calorimeter and add to the jet energy the track momentum.

2 Factors influent on jet reconstruction

Let us consider a factors that influence the reconstructed jet energy. They can be divided into two groups. One is connected with the physics of an object such as a jet:

- fragmentation model of jet
- initial and final state radiation
- underlying event-particles coming from other interacting partons.
- in the case of pile-up, the particles coming from additional minimum bias events.

The other factors related to the detector performance are following :

- electronic noise
- magnetic field which deflects low energy charged particles out of the jet reconstruction cone
- different response of em and hadronic particles
- losses due to out of cone showering
- dead materials and cracks
- longitudinal leakage for the high energy jets

CMS calorimeter consists of two different compartments which have different response for the em and hadronic particles. The non-linearity of the HCAL is 15 % as it was shown in the test beam over the momentum range 20 to 300 GeV [6]. The ratio of the beam energy to the reconstructed energy is presented in Figure 1, assuming that for the electrons this ratio is equal 1 in the whole dynamic range.

The correction for the effects in the first group should be left for the concrete physics channel investigations. As for the detector effects, they could be considered more or less independent of the physics channel. Common correction coefficients can therefore be provided.

3 Energy corrections for calorimeter jets

Algorithms for the jet energy corrections are considered as follows :

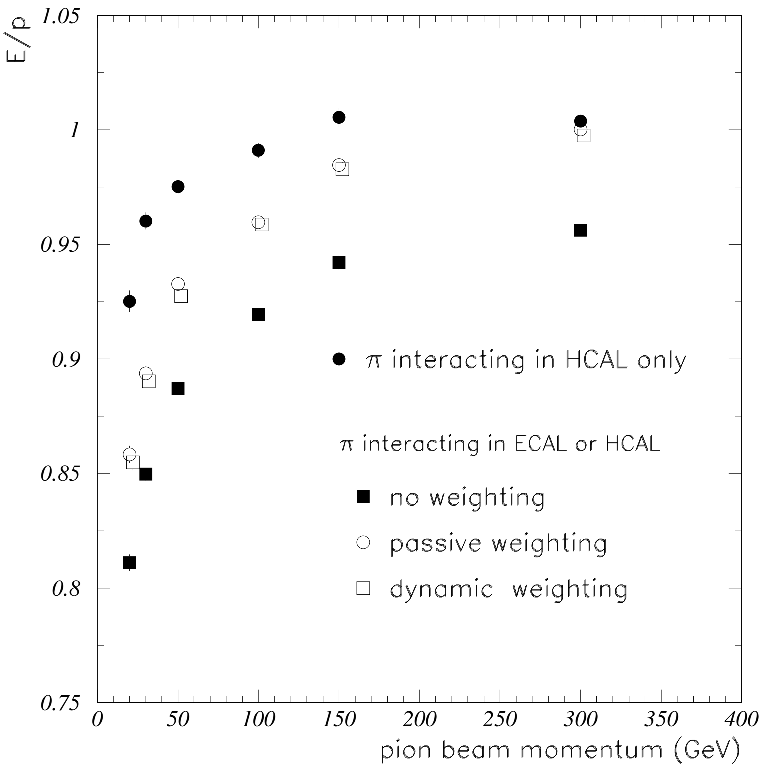

Figure 1: Linearity of HCAL and ECAL+HCAL response from the test beam data [6]

- jet based.
  Corrections are implemented by weighting the measured energy in the longitudinal compartments of the calorimeter.

$$E = a \times (EC + HC) \tag{1}$$

  or

$$E = a \times EC + b \times HC \tag{2}$$

  These weights (a,b) depends on (η, E_T) and are tuned for the objects they are referred to (jets of different origin, Missing Et, etc).

- Cluster based
  E=em+had, calibration coefficients are applied separately to electromagnetic cluster and hadronic clusters.

- Use of reconstructed tracks
  The main idea is to replace the energy of the calorimeter cluster produced by the charged track by the momentum of track in tracker.
  1) Energy of jet gathered inside the jet reconstruction cone does not include the tracks that are swept out of the cone due to the magnetic field. After reconstruction of these tracks, the sum of their momenta, labeled $E_{out\ of\ cone}$ can be added to the jet response $E_{in\ cone}$ in the calorimeter.
  E_{jet}=$E_{in\ cone} + E_{out\ of\ cone}$
  In the case of a good track-calorimeter cluster matching replace the cluster energy by the track momentum.

  2) For all the charged reconstructed tracks one can use their measured momenta in the tracker and subtract the expected response of these particles from the jet energy response in the calorimeter. Then the energy of jet is considered as sum of responses of $e\gamma$ and neutral hadrons and momenta of charged hadrons:

  E_{jet}=EC(e/γ)+(EC+HC)(neutral hadrons) + Tracks (charged hadrons).

4 Detector description

4.1 Calorimeter segmentation

In the barrel and the most of the endcap part of HCAL, the size of the towers is $\Delta\eta = 0.0870$ by $\Delta\phi = 2\pi/72 \approx 0.0873$. At high η in the HCAL endcap ($\eta > 1.74$), the towers become larger in η and double in size in ϕ. The granularity of crystals in the ECAL barrel is $\Delta\eta \times \Delta\phi = 0.0175 \times 0.0175$ which corresponds to a crystal front face $\simeq$ 20×20 mm^2. In the ECAL endcap ($1.48 < |\eta| < 3.0$) the η, ϕ granularity increases progressively to a maximum value of $\Delta\eta \times \Delta\phi = 0.05 \times 0.05$, while the crystal size remains the same (front face $\simeq$ 30×30 mm^2). There is no longitudinal segmentation in the ECAL and the barrel part of the HCAL. The HCAL endcap has 2 or 3 segments in depth but it has not been exploited in the present study.

CMS calorimeter responses were simulated using detailed calorimeter description in GEANT3 (CMSIM120 [12]). For the reconstruction of the energy deposition in the hadron calorimeter calibration constants [13] obtained for the hadron shower model GHEISHA (in GEANT3) have been used. They have been determined with E_t= 50 GeV pions at $0.05 < \eta < 0.3$ for the barrel and $1.8 < \eta < 2.2$ for the endcap part of the calorimeters. The GEANT cuts were 1 MeV for electrons and photons and 10 MeV for hadrons.

4.2 Tracker detectors

Starting from the beam axis the tracker is composed from two different types of the detectors: the pixel layers and the silicon strip counters. The pixel detector consists of 3 barrel layers located at 4, 7, 11 cm from the beam axis with granularity $150 \times 150\mu m^2$ and 2 forward layers with granularity $150 \times 150\mu m^2$ located at a distance 34 and 43 cm in Z from the center of detector.

Silicon strip detectors are separated into inner and outer sections and fill the tracker volume from radii of 20 cm to 110 cm (10 layers) in transverse direction and up to 260 cm (12 layers) in the longatudinal direction. The strip length for the silicon strip counters varies from 10 cm up to 21 cm for the outermost layers and the pitch varies from 61 to 205 μm depending on radii.

5 Energy flow in CMS

We describe below an algorithm for building the energy flow objects with the CMS calorimeter and tracker proposed originally in [5]. A first performance studies of the energy flow method made in [5] looks very promising. Here we present an updated result on dijet mass reconstruction for $Z' \to$jj events using energy flow objects.

5.1 Building of the energy flow objects

5.1.1 Calorimeter clusters

The transverse size of the clusters produced by the charged pions has been analysed from the test beam data [6] with a setup close to that proposed for CMS. It was found that the most of the energy of pions interacting in the ECAL is contained in 3×3 array of crystals and 3×3 array of HCAL towers behind ECAL. Transverse shape in 3×3 array of crystals (for example weighted transverse radius) does not allow an effective discrimination between pions interacting in the ECAL and electrons. Information in the HCAL behind ECAL cluster is then used for electron(photon)/pion discrimination when energy flow objects are build.

The clustering begins in the electromagnetic calorimetry, ECAL, as it has the finest granularity. Crystals are ordered in transverse energy, E_t. The largest E_t crystal serves as a seed for the cluster. Additional crystals are added to the cluster in 3×3 array centered on the seed crystal. All crystals with E_t above 0.1 GeV are accepted. The ECAL clustering is terminated when the seed crystal transverse energy falls below 0.2 GeV. All crystals that participate in a cluster are removed from the further clustering.

The information in depth was used to sort the ECAL clusters into two categories. Energy in the hadronic calorimeter compartment (HCAL) behind the ECAL seed in a 3×3 HCAL tower array is added if the HCAL transverse energy in greater than 30 % of the ECAL cluster energy. This value was picked using test beam data [6] for pions interacting in the ECAL compartment. If there was no HCAL deposit, then the cluster was considered to be a neutral particle (photon or electron), flag = 0. If there was a match, the cluster was considered to be a charged or neutral hadron which interacted in the ECAL compartment.

When the ECAL energy is exhausted, the remaining HCAL energy is ordered in E_t. The seed in HCAL (HCAL tower) has adjacent 3 $\times$ 3 HCAL towers clustered similarly to the ECAL clustering. The process is terminated when the seed tower E_t falls below 0.2 GeV.

The result of this clustering is a cluster energy, E_t weighted centroid in (η, ϕ), and a particle flag. The flag is 0 if the ECAL cluster has no associated HCAL energy. It is 1 if there is associated HCAL energy of at least 30 % of the ECAL energy. Finally, the flag is 2 if there is only HCAL energy without sufficient associated ECAL energy. The last category is assumed to a charged or neutral hadron interacted only in the HCAL.

5.1.2 Cluster-track matching

The tracks used in this study are not reconstructed tracks but the PYTHIA generated charged particles. Given that the tracking momentum resolution is much better than the calorimeter energy resolution this approximation should not alter the qualitative conclusions which are made.

Only tracks with $|\eta|$ <2.4 and transverse momentum, p_t greater than 1 GeV are considered. These cuts approximate the angular coverage of the CMS tracker and the lowest transverse momentum not curled up by the magnetic field (loopers). The "looper" transverse momentum to strike ECAL is 0.78 GeV.

Deviation of the swum tracks from the calorimeter clusters is calculated taking the impact error to be 0.087 (HCAL tower size) for both ϕ and η. Matching in energy assumes a dominant calorimeter error with a 100 % stochastic term and a 5 % constant term [6]. Tracks that are within the calorimeter impact resolution (tower size) in η and ϕ at the HCAL radius are first merged and their momenta added when considering a match to a calorimeter tower. This procedure allows matches in the dense core of jets where charged tracks overlap within a calorimeter tower.

A match between the calorimeter cluster and the tracks is defined to exist if $|\Delta\eta|$ is less than 1 (deviation normalised to HCAL tower size), if $|\Delta\phi|$ is less than 2 and if the difference between track momentum and calorimeter cluster energy, normalised to calorimeter resolution (Δ)E, is between -1 and 3. The offset is due to the observation that the calorimeter energies are systematically lower than the track momenta. In the case of multiple matches, the match with the lowest "chi squared" is taken. If a match exists in all three kinematical variables ($|\Delta\eta|$, $|\Delta\phi|$, ΔE) the calorimeter cluster is replaced by the matching track. A new flag is defined to be 3 if this replacement is made. Tracks which would never reach the barrel, "loopers", are added back into the "energy flow" list and a flag = 4 is set.

The end result is an energy flow list consisting of unmatched calorimeter clusters (flag = 0, 1 or 2), matched (merged) tracks (flag = 3), and tracks which would not reach barrel calorimeter (flag = 4).

5.2 Dijet mass reconstruction with energy flow objects

The data set to test the energy flow method was 120 GeV hypothetical Z' bosons decaying into light quarks with initial state and final state radiation turned on. Events were fully simulated in cms120 and digitised in ORCA5 for $L = 2 \times 10^{33} cm^{-2} s^{-1}$. The tracks used in this study were not reconstructed tracks but the PYTHIA generated charged particles. These tracks are swum in a uniform axial magnetic field to a radius corresponding to the front face of the HCAL. The event by event z position of the vertex is used in the swiming.

The data used for dijet mass reconstruction were either calorimeter clusters or a hybrid energy flow set consisting of unmatched clusters plus matched tracks and track loopers. The largest E_t cluster served as a seed for the first jet. The next highest E_t cluster at distance $>$ 2R from the first seed was defined to be the seed for the second jet. The vector sum of all the fragments defined the momentum of the jet. The clusters were assumed to be massless. The dijet mass was calculated for the two largest transverse momentum clusters. The calculation was done both for pure calorimeter clusters and for the energy flow list consisting of unmatched clusters, matched tracks, and barrel loopers. Cone size R=0.9 was taken for the jet energy reconstruction.

The distribution in dijet mass computed using only calorimeter clusters is shown in Fig. 2. The distribution calculated using all, the available information from calorimetry and tracking is shown in Fig. 3. Gaussian fits were made to the histogrammed data. The mean and sigma for the reconstruction with the calorimeter clusters only are $< M_{jj} >$=81.7 $\pm$ 1.1 GeV and $\sigma_{M_{jj}}$ = 17.1 $\pm$ 1.0 GeV. The mean value is different from 120 GeV since no energy corrections have been applied to calorimeter clusters. For the reconstructin with energy flow objects the values are $< M_{jj} >$=105.5 $\pm$ 1.4 GeV and $\sigma_{M_{jj}}$ = 17.8 $\pm$ 1.1 GeV. We can conclude that mass resolution is improved from 21.0 % to 16.9 % with the usage of the energy flow objects.

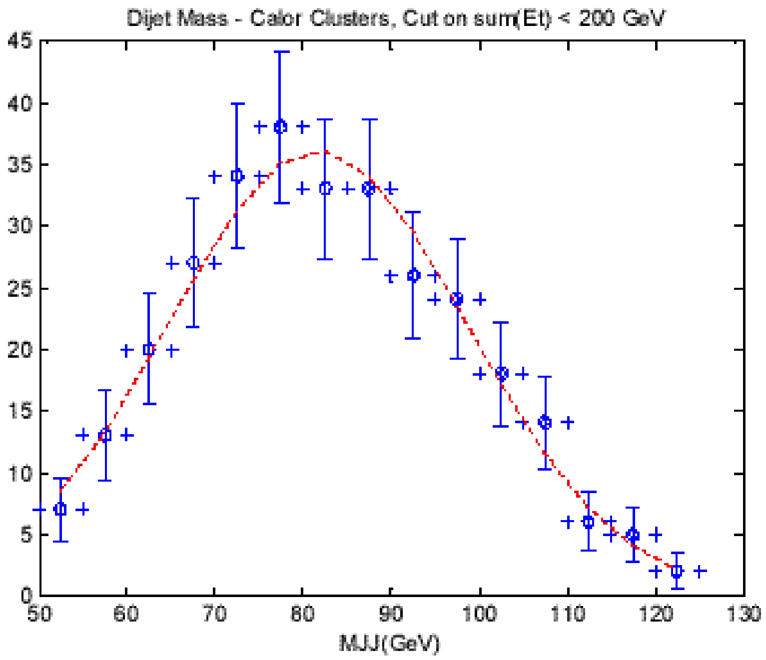

Figure 2: Dijet mass for $Z' \rightarrow$jj events ($M_{Z'}$=120 GeV) reconstructed with calorimeter clusters

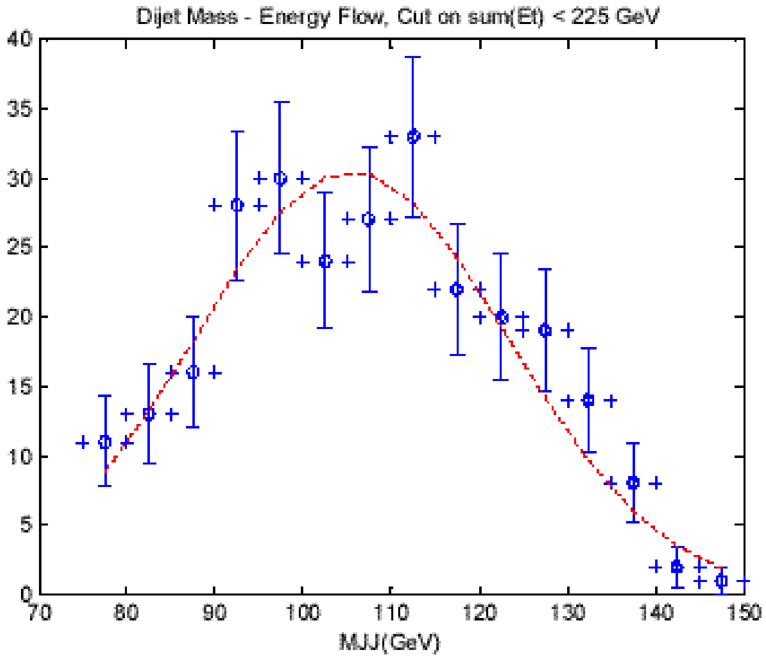

Figure 3: Dijet mass for $Z' \rightarrow$jj events ($M_{Z'}$=120 GeV) reconstructed with the energy flow objects : unmatched clusters, matched tracks and unobserved track loopers.

The energy flow method may also be very useful in improving missing transverse energy resolution. This will be tested in the future. This will require reconstruction of all the tracks in the event.

6 Jet energy measurement with the regional usage of tracks

Some physics may not require global track finding which is expected to be time consuming, but rather a track reconstruction in a region of interest, for example around the axis of the calorimeter jet(s) with not too big cone size. Such tracks can be used to improve the jet energy resolution. As a possible application one may consider $h \to b\bar{b}$ events in associated Higgs production with $t\bar{t}$ [7], [8].

We consider here the case when a jet is found first with a "standard" jet finder running on calorimeter towers as an input. The algorithm for the usage of tracks found with a regional track finder around the calorimeter jet axis can be broken into three steps :

- addition of tracks swept outside the jet reconstruction cone in the 4T field.
- replacement of the cluster energy inside the jet reconstruction cone by the track momenta if there is a good track-cluster matching.
- subtraction of the average expected calorimeter responce of the track from the jet energy for the bad track-cluster match and adding of the momentum of the track

We have tried in this algorithm slightly different criteria to define the calorimeter cluster and track-cluster matching than ones described in the energy flow chapter.

6.1 Addition of out-of-cone tracks

Relatively soft p_t tracks can be swept away from the jet reconstruction cone by the 4T magnetic field. For example a track with p_t=1.6 GeV (produced in the pp interaction) is deflected by the magnetic field by $\Delta\phi$ = 0.5 radian from the original direction when it reaches the ECAL calorimeter. Tracks with $p_t \leq$ 0.8 GeV don't reach barrel calorimeter at all. In this chapter we describe a first step towards full usage of tracks in the jet energy measurement : adding energy of the out-of-cone tracks measured with the tracker to the the energy of the jet measured with the calorimeter. We define an out-of-cone track as a track satisfying the following criteria:

- $\Delta R_v < R_{reco}$,
- $\Delta R_c > R_{reco}$,

where R_{reco} is the cone size used for the jet finding, ΔR_v is the distance in η, ϕ space between the calorimeter jet axis and the track direction at the production vertex, ΔR_c is a distance between jet axis and the expected impact point of the track on the calorimeter surface.

6.1.1 Simulated data

The effect of addition of the out-of-cone tracks on the jet energy resolution has been studied using QCD 2-jet events generated with Pythia 6.152 [9] MSEL=1 subprocesses and in $\hat{p}_t$ bin 50-80 GeV. Pythia settings can be found in [10]. Events have been passed through full detector simulation with cms120 and digitized with the ORCA5 [12] package at a luminosity $L = 2 \times 10^{33} cm^{-2} s^{-1}$. The highest E_t calorimeter jet reconstructed in ORCA with Iterative Cone algorithm using a cone size of R_{reco}=0.5 is used to test the effect of the addition of out-of-cone tracks. We define a generated jet as a bunch of the generated particles from the hard $\hat{p}_t$ interaction where each particle has $\Delta R_v < R_{reco}$ (ΔR_v and R_{reco} are defined in the previous chapter). Fig. 4 shows the average p_t of charged particles in the generated jet as a function of the generated jet transverse energy for the jets with $|\eta_{jet}| <$ 0.5. Fig. 5 shows an average number of charged particles in the Monte Carlo jet as a function of generated jet transverse energy for the jets with $|\eta_{jet}| <$ 0.5. Fig. 6 presents the fraction of energy of the generated jet escaping out of the jet cone. One can see that on average about 15 % of the energy of the soft ($\sim$ 30 GeV) jets escapes from the jet cone and there are a big fluctuations of this energy. Addition of the energy of the out-of-cone tracks into the calorimeter jet energy may remove these fluctuations and therefore improve jet energy resolution. The size of a such improvement is discussed in the following two chapters.

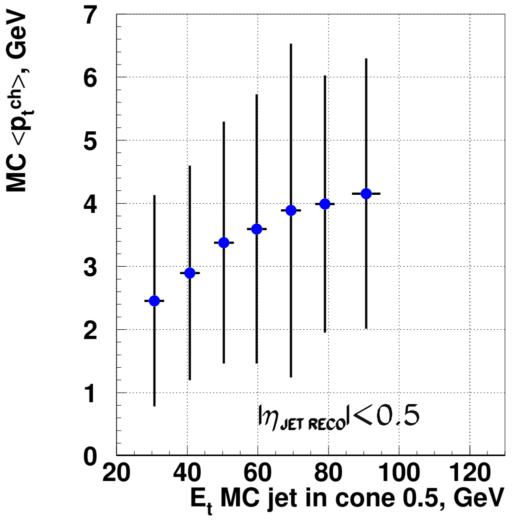

Figure 4: Average p_t of generated charged particles inside a jet cone of ΔR=0.5 as a function of generated jet transverse energy

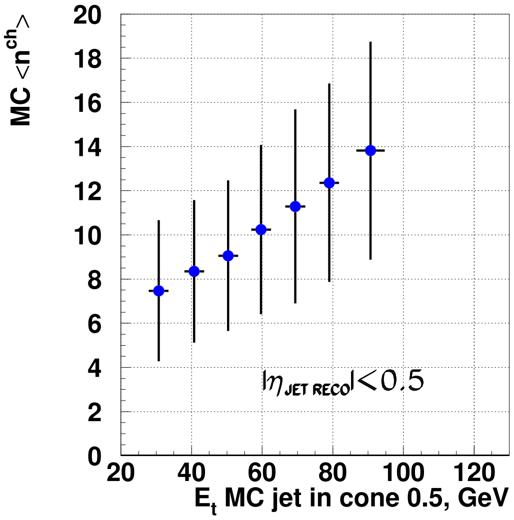

Figure 5: Average number of generated charged particles inside jet cone ΔR=0.5 as a function of generated jet transverse energy

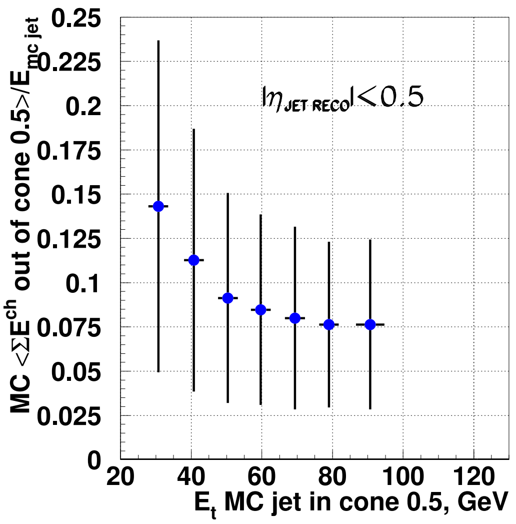

Figure 6: Fraction of energy of the generated jet escaping from the jet cone ΔR=0.5 in 4T field.

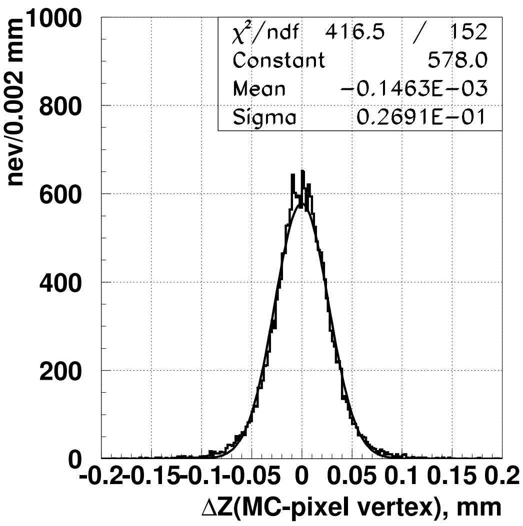

Figure 7: Difference in the Z coordinate between the generated vertex and the reconstructed primary vertex (PV)

6.1.2 Algorithm to add out-of-cone tracks

The algorithm presented below uses tracks reconstructed from the "pixel line" seeds. Only the pixel lines from the primary vertex are considered as seeds for the track finder. A pixel line is defined as a track reconstructed with the pixel detector only. The algorithm for the pixel line reconstruction and vertex finding with the pixel lines is described in [15]. For the track reconstruction we use Combinatorial Track Finder with default settings [16]. The reconstructed primary vertex (PV) is defined in this study as a vertex with maximal $\Sigma|p_t^i|$ of the pixel lines attached to the vertex. Fig. 7 shows the difference in Z coordinate (ΔZ) between generated vertex and PV defined with the pixel lines as described above. One can conclude from the absence of the tails in ΔZ distribution that in almost all cases there is a correct assignment of the pixel signal vertex with the generated signal vertex. The resolution in Z coordinate is about 30 μm.

The present algorithm steps to add out-of-cone tracks are the following :

- reconstruct all pixel lines and vertices from the pixel lines.
- use pixel lines from the PV that are within the cone R_{reco} (cone size for the calorimeter jet finder) around the calorimeter jet direction as seeds for the Combinatorial Track Finder.
- find impact points of the reconstructed tracks on the surface of the calorimeter (ECAL)
- add to the calorimeter jet energy the scalar sum of p (momentum) of the tracks with impact points outside of the jet reconstruction cone and recalculate η, ϕ of the jet taking into account added tracks.

Fig. 8 shows the p_t spectra of the generated charged particles (solid line) and reconstructed tracks (dashed line) inside cone R_{reco}=0.5 around jet axis. The efficiency of reconstruction for tracks with $p_t > 0.9$ GeV is shown in Fig. 9.

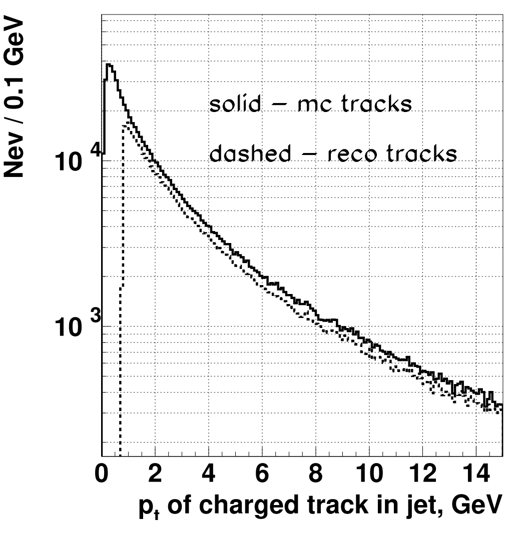

Figure 8: p_t spectra of generated charged particles (solid line) and reconstructed tracks (dashed line) inside jet cone 0.5

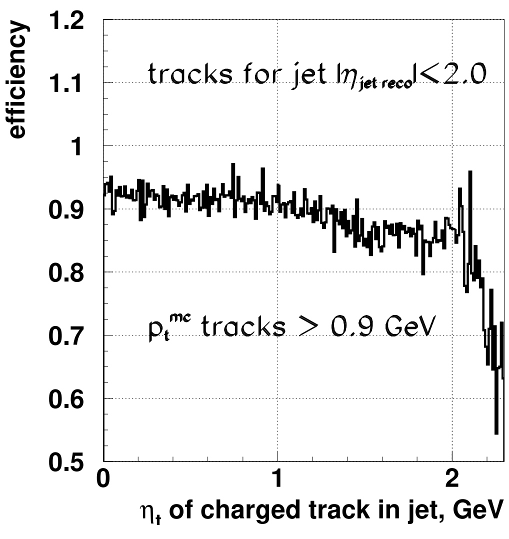

Figure 9: Efficiency of reconstruction of the tracks ($p_t > 0.9$ GeV) inside jet cone of ΔR=0.5 as a function of jet pseudorapidity.

6.1.3 Results

Fig. 10 shows transverse jet energy resolution as a function of E_t of the generated jet with $|\eta_{jet}| < 0.5$ for three cases: dots - calorimeter jet energy resolution; squares - with addition of the generated out-of-cone tracks of any p_t; triangles - with addition of the reconstructed out-of-cone tracks. One can see that the addition of the momentum of out-of-cone tracks improves jet E_t resolution by about of 10-15 % and the improvement is more visible for softer

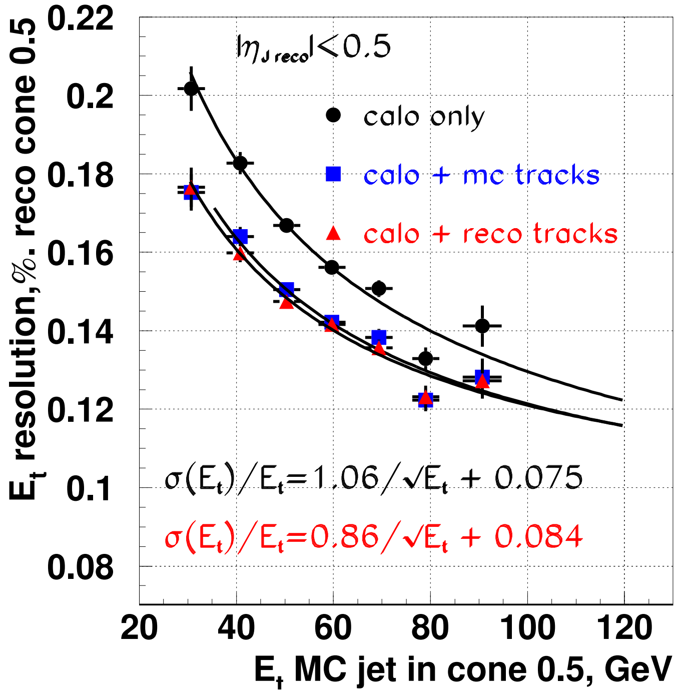

Figure 10: Jet energy resolution with calorimeter only - black points, after adding out-of-cone generated charged tracks - blue points, after adding of out-of-cone reconstructed tracks - red points. Jets are considered with $|\eta| < 0.5$.

jets. Improvement is almost the same when the generated or reconstructed tracks are used. It means first, that the usage of the very soft tracks of $p_t < 0.9$ GeV does not improve further the jet E_t resolution and the second, that the track finding inefficiency is low enough so as not to degrade the performance of this algorithm. Fig. 11 and Fig. 12 show the jet E_t resolution for jets in pseudorapidity regions $1.0 < |\eta_{jet}| < 1.5$ and $1.5 < |\eta_{jet}| < 2.2$. One can see that the improvement of the resolution is more visible in the barrel part of the calorimetry $|\eta_{jet}| < 1.5$ which can be explained by the fact that the bigger fraction of the jet energy escapes reconstruction cone in the barrel than in the end cap. Formulas shown in Fig. 10, Fig. 11 and Fig. 12 are parameterisations of the jet E_t resolution.

6.2 Cluster-track matching and algorithm for subtraction of associated energy

6.2.1 Simulated data

Samples of QCD dijet events in a different intervals of $\hat{p}_t$ were simulated with Pythia 6.152 [9] using settings [10], which include:

• The parton density structure function CTEQ 5L,

• Pythia generation datacards (Table 1).

Table 1: Pythia generation datacards for minimum-bias events.

MSEL = 1	Non-diffractive (jet) processes
MSTP(2) = 2	2nd order runnings α_s
MSTP(33) = 3	K-factors: fixed and α_s scale shift at PARP(33) = 0.075 * Q^2
MSTP(82) = 4	Multy-parton interactions switched on
MSTP(81) = 1	Multy-parton interactions switched on
PARP(82) = 3.2	regularization scale $p_{\perp 0}$ of the transverse momentum spectrum for multiple interaction with MSTP(82) ≥ 2

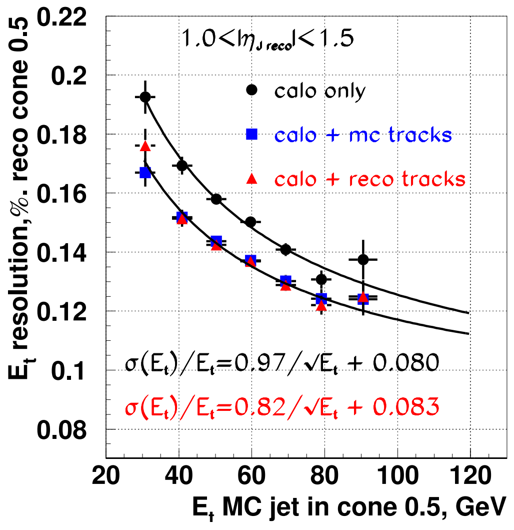

Figure 11: The same as in Fig. 10 for jets with 1.0 $< |\eta| <$ 1.5

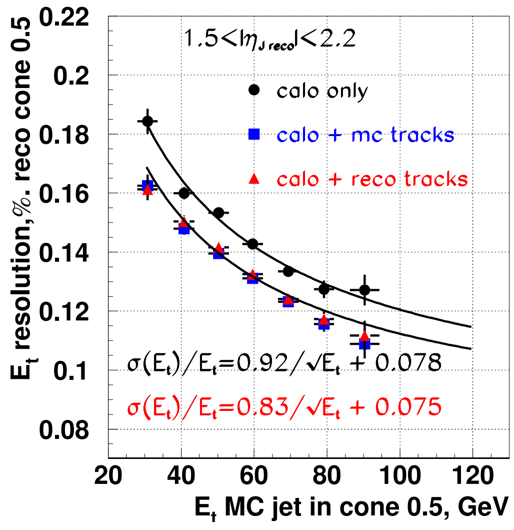

Figure 12: The same as in Fig. 10 for jets with 1.5 $< |\eta| <$ 2.2

Jets were found first at the generation level (stable particles, including muons and neutrinos) with a simple cone algorithm PYCELL and a cone size ΔR=0.5. These jets will be refered as Monte-Carlo jets (MC jets). Only one MC jet is taken and the particles which belong to this jet are passed through detector simulation; other particles in QCD event were ignored. Therefore, we mainly pay attention to the detector effects excluding the effects of the initial and the final state radiation as well as underlying and pile-up events. Calorimeter hit digitization has been done with cmsim for no pile up scenario. Calorimeter level jets were reconstructed using a cone of size Δ=0.5 (as MC jets) using the default calorimeter calibration on the single pion as descibed above.

6.2.2 Algorithms and results

To start with the generated charged particles from the PYTHIA are used. The algorithm steps are the following :

- a jet is found in the calorimeter (R jet) using a cone of size ΔR=0.5.
- All charged tracks in cone 0.5 around the calorimeter jet axis are propagated in the magnetic field until they reach the calorimeter surface.
- a matrix of 3$\times$3 crystals and 3$\times$3 HCAL towers is built around the entry point of the charged track.
- the sum of the energy from 3$\times$3 crystals and 3$\times$3 HCAL towers is compared if it is coincided with the momentum of the charged track found in the tracker. If the difference lies within the following window :

$$-\sigma < (Etracker - Ecalo) < 2\sigma \tag{3}$$

  where

$$\sigma/E = 100\%/sqrt(E) + 5\% \tag{4}$$

  the energy is replaced by the track momentum from tracker. The procedure begins from the highest momentum track.

- If the track is not matched (condition for matching is not satisfied) then we calculate the expected response of this track in the calorimeter and subtract it from the Rjet and add the momentum of the charged track instead.

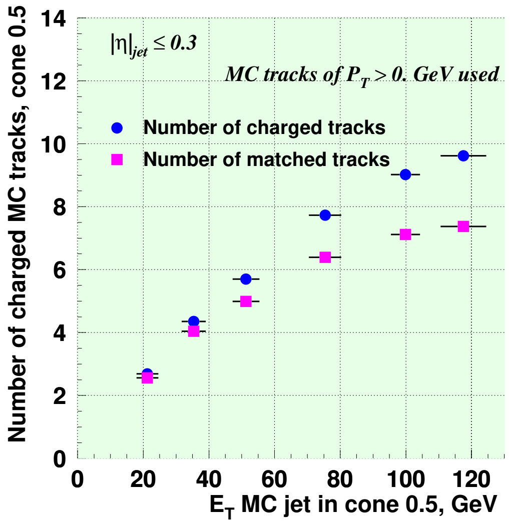

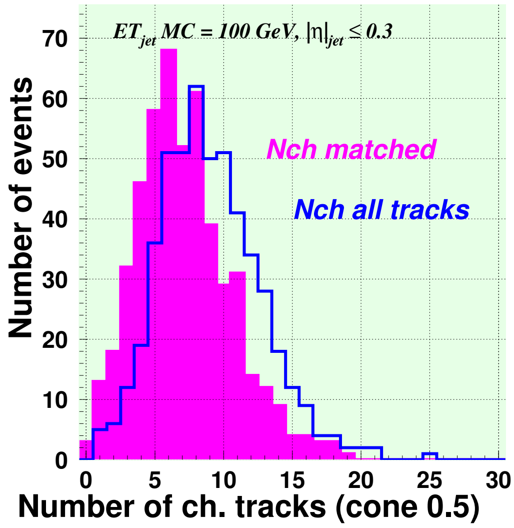

Figure 13: The mean number of charged particles entering into calorimeter reconstruction cone of size ΔR=0.5 (dots) and mean number of matched tracks (squares) as a function of the MC jet energy.

Figure 14: Distribution of the number of impacts from charged particles within calorimeter reconstruction cone of size ΔR=0.5 (left histogram) and mean number of matched tracks (right histogram) for 100 GeV MC jet.

The mean number of matched tracks as a function of MC jet energy is shown in Fig. 13. For the low energy jets the charged tracks are more separated. Therefore, fewer cluster overlaps occur and thus more clusters can pass the matching criteria.

The distribution of the number of matched and number of charged tracks for the 100 GeV jets is shown in Fig. 14.

Two different methods have been tried to evaluate the expected response of the charged track in the calorimeter and both are based on the measurements from single or isolated particles.

- one can calculate the expected response from e/π ratio of the charged hadrons measured for different energy with a set of isolated particles [11]. This can be done during data taking. We also should evaluate the ratio of energy that particle leaves in ECAL and HCAL. The response in ECAL is different if particle has interacted in ECAL or not. We separate interacting and non-interacting particles using the energy deposited in 3×3 crystals; if $E_{3\times3}$ <0.5 GeV the particle is classified as non-interacting. The expressions for the expected response for charged particles are given in Table 2.

Table 2: Expected response for charged particles.

	Particle interacts in ECAL	Particle does not interact in ECAL
R_{ECAL}	$Etrack * 0.4/(e/\pi)_{ECAL}$	E_{MIP}
R_{HCAL}	$Etrack * 0.6/(e/\pi)_{HCAL}$	$(Etrack - E_{MIP})/(e/\pi)_{HCAL}$

The e/π ratio in ECAL and HCAL is calulated with expressions [11]:

$$(e/\pi)_{ECAL} = (e/h)_{ECAL}/(1 + ((e/h)_{ECAL} - 1) \times F0_{ECAL}) \tag{5}$$

$$(e/\pi)_{HCAL} = (e/h)_{HCAL}/(1 + ((e/h)_{HCAL} - 1) \times F0_{HCAL}), \tag{6}$$

where $(e/h)_{ECAL} = 1.6$, $(e/h)_{HCAL} = 1.39$ are obtained by fitting test beam data for 300 GeV pions [11]. $F0_{ECAL}$, $F0_{HCAL}$ are the electromagnetic fraction of hadronic showers and can be estimated using: $F0_{ECAL/HCAL} = 0.11 \times ln(E_{ECAL/HCAL})$ [11]. The ratio $E_{ECAL}/E_{HCAL} = 0.4/0.6$ was obtained from the analysis of the test beam data for 300 GeV pions [17]. Although the value of the ratio E_{ECAL}/E_{HCAL} depends on the energy of particle we use a constant value in our calculations for the moment.

- Library of responses

  The mean responses in ECAL and HCAL corresponding to interacting and non-interacting particles found using a set of isolated particles of different energies. Initial energy of particles is taken from the tracker reconstruction. The dependence of the mean responses in ECAL and HCAL are shown in figure 15 and 16 for isolated particles interacting in ECAL and in figure 17 for non-interacting particles in ECAL.

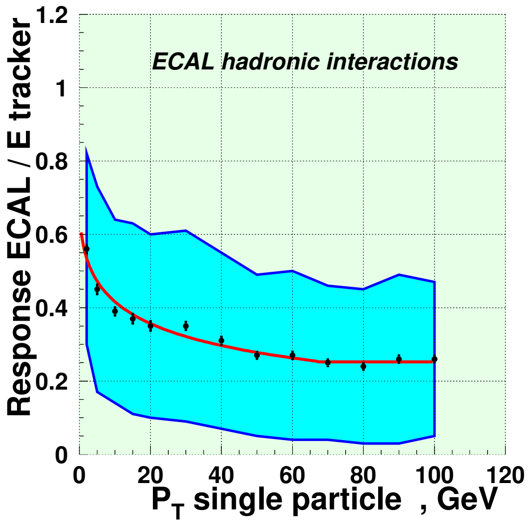

Figure 15: The mean response in ECAL for isolated charged particles interacting in ECAL as a function of particle p_t. The shadowed area corresponds to dispersion of 1 σ.

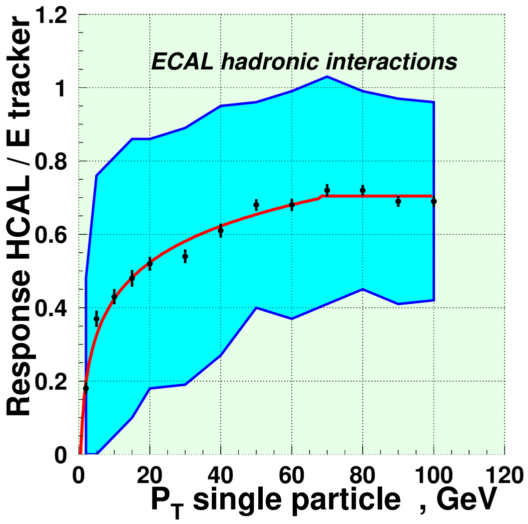

Figure 16: The mean response in HCAL for isolated charged particles interacting in ECAL as a function of particle p_t

Finally the energy of out-of-cone tracks is also added to the energy of jet. The dependence of jet energy resolution and jet energy linearity on the MC jet energy is presented in Fig. 18 and Fig. 19 for the four different cases. The first one corresponds to the case when only the expected response subtraction procedure is used and expected response is evaluated using the e/π. In the second case the expected response is calculated from the library of responses and in the third case full correction with track matching, library of responses and out-of cone tracks is performed. Open circles correspond to the case where only the out-of-cone tracks are added to the calorimeter energy. Including only out-of-cone tracks gives already half of the possible improvement. Different correction by exchanging the response of charged tracks with the energy gives the same improvement for resolution, but the best linearity can be achieved with track-cluster matching, library of responses and tracks out of cone.

7 Conclusions

We have proposed and tested the performance of the two algorithms which use tracks to improve the CMS calorimeter energy resolution.

The energy flow algorithm builds a list of objects consisting of unmatched calorimeter clusters, matched tracks, and barrel loopers (tracks which don't reach barrel calorimeter surface). A method of discrimination between calorimeter clusters produced by electrons or photons and hadrons using HCAL energy behind ECAL cluster has been proposed. The track-cluster matching criteria have been developed to replace of the calorimeter cluster energy by matched track momentum. The performance of the algorithm has been tested by reconstructing the dijet mass of 120 GeV Z's decaying into two jets. It has been shown that dijet reconstruction with energy flow objects improves

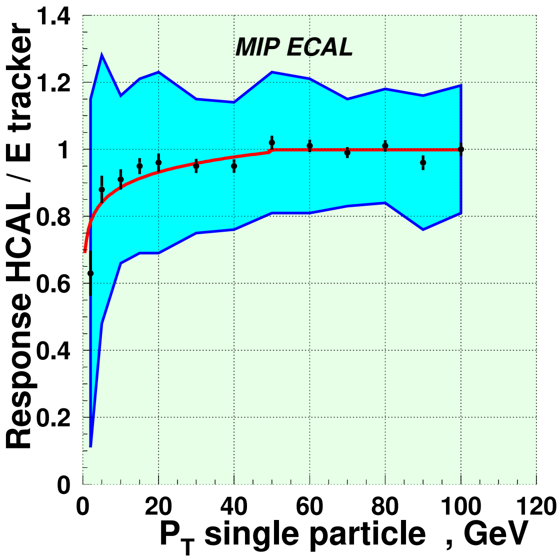

Figure 17: The mean response in HCAL for isolated charged particles non-interacting in ECAL as a function of particle p_t.

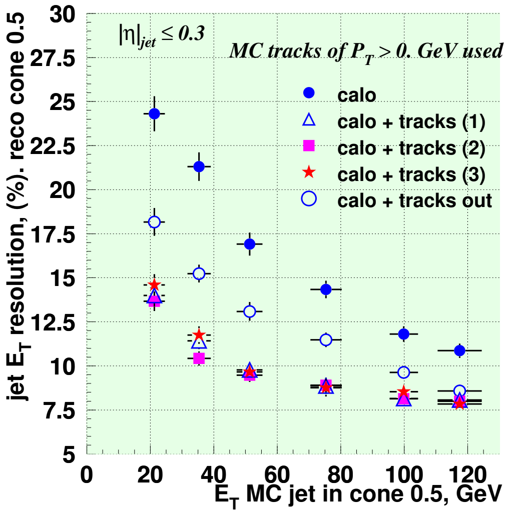

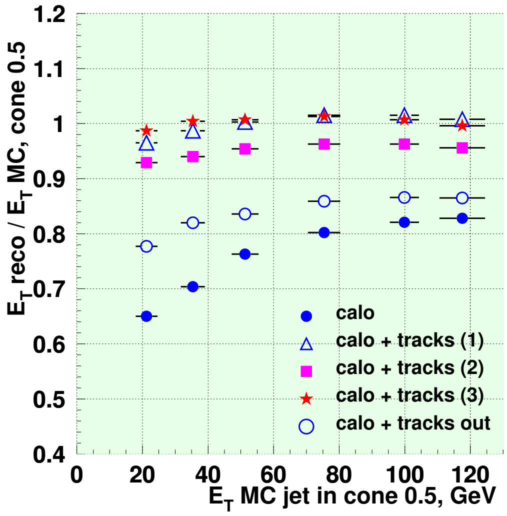

Figure 18: The dependance of jet energy resolution on generated jet energy: only calorimeter responses used (closed circles), out of cone tracks added to calorimeter responses (open circles), subtraction procedure of expected responses using e/π technique and out of cone tracks (open triangles), subtraction procedure of expected responses using library of responses and out of cone tracks (closed squares), matched tracks and library of responses and out of cone tracks (close stars)

Figure 19: The dependance of reconstructed jet energy on generated jet energy. The points are the same as in figure 18

by about 22 % the dijet mass resolution in comparison with using of only the calorimeter clusters. Generated tracks are still used for this study. The energy flow method may also be very useful in improving the missing transverse energy resolution. This will be tested in the future. This requires reconstruction of the all tracks in the event.

The method of improving the jet energy resolution with regional usage of the tracks has been also proposed when a jet is found first with a "standard" jet finder running on calorimeter towers. It has been shown that the addition of tracks swept out from the reconstruction cone by 4T magnetic field brings already about half of the improvement in the resolution for the soft ($\simeq$ 30-40 GeV) jets. The other half of the resolution improvement comes from the replacement of the calorimeter clusters by the matched track momenta inside the jet reconstruction cone. For the bad track-cluster matching we subtract from the jet energy the expected response of the track in the calorimeter and add to the jet energy the track momentum. It has been shown that the jet energy resolution may be improved by about factor of 2 for the soft jets of $E_t \simeq$ 30-40 GeV. The second part of the algorithm (working inside jet cone) has been tested so far with simplified single jet events and generated tracks and still has to be checked real events and ORCA reconstruction including realistic noise and track reconstruction. This method could be used to improve the dijet mass resolution in multijet events where jet cone size cannot be made too big - for example to improve $h \rightarrow b\bar{b}$ mass resolution when Higgs is produced in association with $t\bar{t}$.

8 Acknowledgments

O.K. and I.V are thankful to L.Sarycheva, N.Kruglov, A.Demianov and A.Gribushin for useful discussions and V.Gavrilov for the interest and support.

References

[1] see for example ALEPH, D. Buskulic et al. NIM A 360(1995) 481-506

[2] S. Lami, A. Bocci, S. Kuhlmann and G. Latino, FERMILAB-Conf-00/342-E CDF January 2001

[3] Matthew Wing, Precise Mesurement of the Jet Energies with the ZEUS Detector, In Proceedings of the IX Int. Conf. on Calorimetry in Part.Phys., Annecy, Oct.9-14, 2000.

[4] P. Gay, Energy flow. In Proceedings of the Linear Collider Workshop 2000, Fermilab, Batavia, IL, USA, 2000. http://www-lc.fnal.gov/lcws2000

[5] D. Green *"Energy Flow in CMS Calorimetry"* Fermilab-FN-0709

[6] V. Abramov et al., NIM, A 457(2001) 75-100.

[7] V. Drollinger "Searching for Higgs Bosons in Association with Top Quark Pairs in the H -¿ bb Decay Mode" CMS Note 2001/054.

[8] D. Green, Kaori Maeshima, Richard Vidal, Weimin Wu "A Study of $t\bar{t}$+Higgs at CMS" CMS Note 2001/039

[9] T.Sjostrand. Comp. Phys. Com. 82/1994) 74.

[10] C.Seez. CERN CMS IN 2000/001.

[11] D. Green, *"Calibration of the CMS Calorimeters"*, Fermilab-FN-704, July 2001.

[12] CMSIM user's Guide at www.http://cmsdoc.cern.ch/swsi.html.

[13] S.Kunori. http://home.fnal.gov/∼kunori/cms_sw/colo_sw/hcal_hits_digi.html.

[14] S.Abdullin et al. *"Energy corrections for QCD jets."* CMS IN 2001/001.

[15] D. Kotlinski *"Track Reconstruction and Primary Vertex Finding using the Pixel Detector Data"* CMS IN 2000/022.

[16] T. Todorov, private communication

[17] J.Freeman, private communication